# DOUBLE-MULTIPLE STREAMTUBE MODEL FOR DARRIEUS WIND TURBINES

Ion Paraschivoiu

Institut de Recherche d'Hydro-Québec
Varennes, Québec
Canada, JOL 2PO

## ABSTRACT

An analytical model is proposed for calculating the rotor performance and aerodynamic blade forces for Darrieus wind turbines with curved blades. The method of analysis uses a multiple-streamtube model, divided into two parts: one modeling the upstream half-cycle of the rotor and the other, the downstream half-cycle. The upwind and downwind components of the induced velocities at each level of the rotor were obtained using the principle of two actuator disks in tandem.

Variation of the induced velocities in the two parts of the rotor produces larger forces in the upstream zone and smaller forces in the downstream zone. Comparisons of the overall rotor performance with previous methods and field test data show the important improvement obtained with the present model.

The calculations were made using the computer code CARDAA developed at IREQ. The double-multiple streamtube model, presented in this paper, has two major advantages: it requires a much shorter computer time than the three-dimensional vortex model and is more accurate than multiple-streamtube model in predicting the aerodynamic blade loads.

## INTRODUCTION

The Darrieus-type vertical-axis wind turbine is one of the best wind energy conversion system. This curved-blade turbine is now under theoretical and experimental study in the U.S., at Sandia Laboratories (2-m, 5-m and 17-m turbines), for example, and in Canada at a larger scale with the 230-kW machine in the Magdalen Islands and, recently a new project for building a prototype of about 4000-kW for the end of 1983.

The first approach to modeling the aerodynamic performance of a Darrieus wind turbine was developed by Templin (ref. 1), who supposed that the rotor is enclosed in a single streamtube.

A more complex analytical model is the multiple-streamtube (ref. 2) in which the swept volume of the turbine is divided into a series of adjacent, aerodynamically independent, streamtubes. The blade element and momentum theories are then employed for each streamtube. This model assumes that the induced velocity varies over the frontal disk area, both in the vertical and the horizontal directions.

Rotor power, torque and drag are calculated by averaging the contributions from each stream-tube. The multiple streamtube model is a good approach for predicting the overall performance and axial force of Darrieus turbines under conditions where the blades are lightly loaded and the rotor tip speed ratios are low, (refs. 2 and 3).

Other types of aerodynamic performance model for studying vertical-axis wind turbines are based on the vortex theory: these are the fixed-wake (ref. 4) and free-vortex models (refs. 5 and 6). Recently, Strickland (ref. 6) extended the free-vortex model to the curved-blade Darrieus turbine, using a concept of the three-dimensional vortex structure. He used a single lifting/line vortex theory to represent an airfoil segment.

Overall turbine performance in the form of drag, torque and power coefficient, have been reasonably predicted by streamtube models and the analytical results are in good agreement with experimental data. The performance values calculated with vortex model in the same conditions (stalled or unstalled blades) are not much better from this point of view. Although the vortex models have the major advantage of predicting the blade forces more exactly than the streamtube models but they have the disadvantage of requiring considerable computer time.

### AERODYNAMIC MODEL

#### Induced Velocities

The calculation of the induced velocities through the rotor is based on the principle of the two actuator disks in tandem at each level of the rotor, as shown in Figure 1. This analytical method uses a multiple-streamtube model divided in two parts: one for the upstream half-cycle of the rotor and the other for the opposite half-cycle (downstream). The multiple-streamtube model has been extended to the flow field upstream and downstream of the rotor.

The upwind and downwind components which traverse each streamtube are considered separately and the variations in the freestream velocity are incorporated into the model. The freestream velocity profile is given by the following relation:

$$V_{\infty 1}/V_{\infty} = \left(Z_i / Z_{EQ}\right)^{\alpha_w} \tag{1}$$

The upwind velocity component is less than the local ambient wind velocity, $V < V_{\infty 1}$, and in the middle plane between the upstream and the downstream zone there is an equilibrium-induced velocity, $V_e < V$; thus the induced velocity decreases in the axial streamtube direction so that the downwind component is less than the equilibrium velocity, $V' < V_e$. Figure 1 shows the velocities induced into a pair of actuator disks in tandem with Lapin's assumption, (ref. 7). For the upstream half-cycle of the rotor, the local
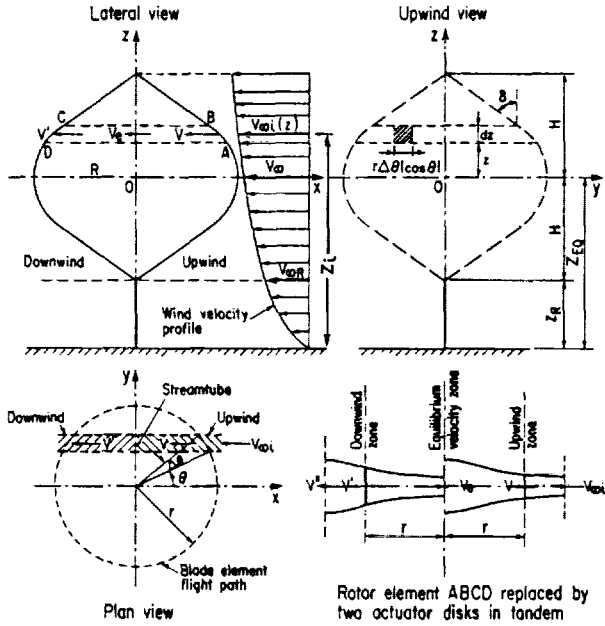
Figure 1 - Definition of rotor geometry for a Darrieus wind turbine. Two actuator disks in tandem.

wind velocity $V_{\infty i}$ decreases by an interference factor of $u \sim 1$ and the induced velocity becomes

$$V = uV_{\infty i} \qquad (2)$$

Finally the equilibrium-induced velocity is

$$V_e = (2u-1) V_{\infty i} \qquad (3)$$

For the downstream half-cycle of the rotor, $V_e$ is the input velocity and, at the end of the stream-tube, the induced velocity can be written

$$V' = u' (2u-1) V_{\infty i} \qquad (4)$$

where $u' = V'/V_e$ is the second interference factor for this part of the rotor, $u' < u$.

Under these conditions, the streamtube induced velocity is calculated by a double iteration, one for each part of the rotor.

### Upstream Half-Cycle of the Rotor

The local relative velocity for the upstream half-cycle of the rotor, $-\pi/2 \leq \theta \leq \pi/2$, is given by the expression:

$$W^2 = V^2 \left[(X - \sin \theta)^2 + \cos^2\theta \cos^2\delta\right] \qquad (5)$$

where $X = \omega r/V$ represents the local tip speed ratio. The definitions of the angles, and the force and velocity vectors at the equatorial plane of the rotor are given in Figure 2. The general expression for the angle of attack is:

$$\alpha = \arcsin \left[\frac{\cos\theta\cos\delta\cos\alpha_0 - (X-\sin\theta) \sin \alpha_0}{\sqrt{(X - \sin\theta)^2 + \cos^2\theta \cos^2\delta}}\right] \qquad (6)$$
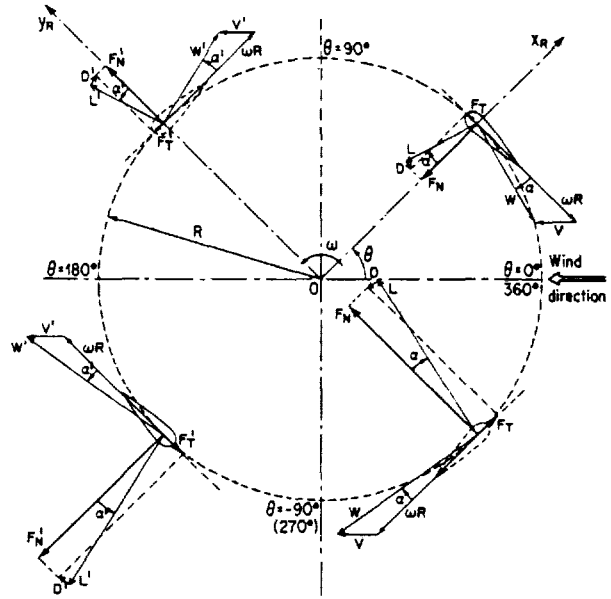
This Equation suggests the possibility of an



Figure 2 - Angles, force and velocity vectors at the equatorial plane.

asymmetrical section or a symmetrical section where the chord line is not tangent to the circle of rotation (or blade flight path), $\alpha_0 \neq 0$, here we supposed $\alpha_0 = 0$.

Using the blade element theory and the momentum equation at each streamtube and by equating the vertical variation of the induced drag coefficient of the rotor, we found:

$$F_{up} (V/V_\infty)^2 = \pi\eta (V/V_\infty) \left[(V_{\infty i}/V_\infty) - (V/V_\infty)\right] \qquad (7)$$

or, in the terms of the interference factor,

$$F_{up} u = \pi\eta (1-u) \quad , \quad \eta = r/R \qquad (8)$$

where $F_{up}$ is the function that characterizes the upwind conditions

$$F_{up} = \frac{Nc}{8\pi R} \int_{-\pi/2}^{\pi/2} \left(C_N \frac{\cos\theta}{|\cos\theta|} - C_T \frac{\sin\theta}{|\cos\theta|\cos\delta}\right)\left(\frac{W}{V}\right)^2 d\theta \qquad (9)$$

and

$$C_N = C_L \cos\alpha + C_D \sin\alpha$$
$$\qquad (10)$$
$$C_T = C_L \sin\alpha - C_D \cos\alpha$$

The blade airfoil section lift and drag coefficients, $C_L$ and $C_D$ respectively, are obtained from NASA and Sandia Laboratories test data by interpolation using both the local Reynolds number and the local angle of attack.

Defining the blade Reynolds number as $Re_b = Wc/\upsilon_\infty$, for local conditions, $Re_b$ is given by the following relation:

$$Re_b = \left(Vc/\upsilon_\infty\right) \sqrt{(X - \sin\theta)^2 + \cos^2\theta \cos^2\delta} \qquad (11)$$

where c is the airfoil chord and $\upsilon_\infty$ is the kine-

matic viscosity. Introducing the turbine Reynolds number $Re_t = \omega Rc/\upsilon_\infty$, we obtain the relationship between $Re_b$ and $Re_t$:

$$Re_b = \left(Re_t \eta/X\right) \sqrt{(X - \sin\theta)^2 + \cos^2\theta \cos^2\delta} \qquad (12)$$

For a given rotor geometry and rotational speed $\omega$ and a given velocity at each streamtube position from Equation (1), a value of induced local tip speed ratio X is chosen by assuming that the interference factor u is unity. Thus, $Re_b$ and $\alpha$ will be evaluated in first approximation and the characteristics of the blade section profile $C_L$, $C_D$. Then, with Equations (10), the normal and tangential force coefficients are estimated, and Equation (9) allows us to evaluate the function $F_{up}$. With the first value of $F_{up}$ we can calculate another value of the interference factor employing Equation (8) and the iterative process is repeated until successive sets of u are reasonably close. Convergence is fast with a maximum number of iterations at the equatorial streamtube, especially for high tip speed ratios, and the error is less than $10^{-4}$. Once the true value of the induced velocity V has been calculated, we can obtain the local relative velocity W with Equation (5) and the effective angle of attack $\alpha$ with Equation (6).

### Upstream Blade Forces and Performance

The streamwise blade force, normal and tangential components may be evaluated for each streamtube as functions of the blade position. Half-rotor torque, power and drag are resolved by averaging the contributions from each streamtube for the upstream half-cycle of the rotor.

For each blade in the upstream position, the non-dimensional force coefficients as functions of the azimuthal angle $\theta$ are given by:

$$F_N (\theta) = (cH/S) \int_{-1}^{1} C_N \left(W/V_\infty\right)^2 (\eta/\cos\delta) \, d\zeta, \qquad (13)$$

for the normal force, and by:

$$F_T (\theta) = (cH/S) \int_{-1}^{1} C_T \left(W/V_\infty\right)^2 (\eta/\cos\delta) \, d\zeta, \qquad (14)$$

for the tangential force, where $\zeta = z/H$ and S is the swept area of the rotor.

The torque produced by a blade element is calculated at the center of each element. By integration along the blade we obtain the torque on a complete blade as a function of $\theta$:

$$T_{up} (\theta) = \frac{1}{2} \rho_\infty cRH \int_{-1}^{1} C_T W^2 (\eta/\cos\delta) \, d\zeta \qquad (15)$$

The average half-cycle of the rotor torque produced by N/2 of the N blades is thus given by:

$$\overline{T}_{up} = \frac{N/2}{\pi} \int_{-\pi/2}^{\pi/2} T_{up} (\theta) \, d\theta \qquad (16)$$

and the average torque coefficient will be:

$$\overline{C}_{Q_1} = \frac{NcH}{2\pi S} \int_{-\pi/2}^{\pi/2} \int_{-1}^{1} C_T \left(\frac{W}{V_\infty}\right)^2 \left(\frac{\eta}{\cos\delta}\right) d\zeta d\theta \qquad (17)$$

Thus the power coefficient for the upstream half-cycle of the rotor can be written:

$$C_{P_1} = \frac{\omega R}{V_\infty} \, \overline{C}_{Q_1} = X_{EQ} \, \overline{C}_{Q_1} \qquad (18)$$

### Downstream Half-Cycle of the Rotor

For the second half-part of the rotor in the streamflow direction (or downstream half-cycle) the local relative velocity is:

$$W'^2 = V'^2 \left[(X' - \sin\theta)^2 + \cos^2 \theta \cos^2\delta\right] \qquad (19)$$

where $X' = \omega r/V'$
and the angle of attack is given by Equation (6) where X is replaced by X' with $\pi/2 \leq \theta \leq 3\pi/2$. The induced velocity in this part of the rotor V' is a function of both interference factors: upstream (u) and downstream (u'), and with the condition of continuity we can obtain one of the velocity components in terms of the others for a certain wind velocity $V_{\infty i}$, Equation (4).

Following the same logic used for the upstream half-cycle, we consider that the equilibrium used for the velocity given by Equation (3) is the input condition of the flow in the downstream half-cycle at each streamtube. Thus, the iterative process is initialized by u' = u, where u is the true value obtained for the first part of the rotor at each level.

The transcendental equation which contains the interference downstream factor u' becomes:

$$F_{dw} u' = \pi \eta (1-u') \qquad (20)$$

where the function $F_{dw}$ is:

$$F_{dw} = \frac{Nc}{8\pi R} \int_{\pi/2}^{3\pi/2} \left(C'_N \frac{\cos\theta}{|\cos\theta|} - C'_T \frac{\sin\theta}{|\cos\theta|\cos\delta}\right)\left(\frac{W'}{V'}\right)^2 d\theta \qquad (21)$$

### Downstream Blade Forces and Performance

The normal force coefficient as a function of $\theta$, for a complete blade, is :

$$F'_N (\theta) = (cH/S) \int_{-1}^{1} C'_N \left(W'/V_\infty\right)^2 (\eta/\cos\delta) \, d\zeta \qquad (22)$$

and the tangential force coefficient of the blade as a function of $\theta$ is given by:

$$F'_T (\theta) = (cH/S) \int_{-1}^{1} C'_T \left(W'/V_\infty\right)^2 (\eta/\cos\delta) \, d\zeta \qquad (23)$$

The torque on a complete blade, in the downstream half-cycle, as a function of $\theta$ is:

$$T_{dw} (\theta) = \frac{1}{2} \rho_\infty cRH \int_{-1}^{1} C'_T W'^2 (\eta/\cos\delta) \, d\zeta \qquad (24)$$

The average half-rotor torque has the following form:

$$\overline{T}_{dw} = \frac{N/2}{\pi} \int_{\pi/2}^{3\pi/2} T_{dw} (\theta) \, d\theta \qquad (25)$$

and the average torque coefficient:

$$\overline{C}_{Q_2} = \frac{NcH}{2\pi S} \int_{\pi/2}^{3\pi/2} \int_{-1}^{1} C'_T \left(\frac{W'}{V_\infty}\right)^2 \left(\frac{\eta}{\cos\delta}\right) d\zeta d\theta \qquad (26)$$

The power coefficient for the downstream half-cycle of the rotor becomes:

$$C_{P_2} = \frac{\omega R}{V_\infty} \overline{C}_{Q_2} \qquad (27)$$

The power coefficient for the full cycle is the weighted sum of the coefficients for the half-cycles:

$$C_P = C_{P_1} + C_{P_2} \qquad (28)$$

## RESULTS AND DISCUSSION

In order to verify this analytical model, we calculated the aerodynamic loads of the blades and torque as a function of the blade angular position as well as the power coefficient as a function of tip speed ratio, including the effects due to ambient windstream shear. The theoretical results obtained with the double-multiple-streamtube were compared with other analytical models such as multiple-streamtube and two-dimensional vortex theory, and with the experimental data for Sandia 5-m rotor (ref.8). The rotor of this turbine possesses two (or three) of the straight-line / circular-arc form, with a constant symmetrical airfoil NACA-0015, from hub to hub.

The double-multiple-streamtube model shows important retardation of the flow in the downwind zone of the rotor. The aerodynamic forces on the blades are considered as the nondimensional normal and tangential force coefficients for each element of the blade, separately, in the upwind and downwind positions. The elemental force coefficients were integrated along the length of the blade and the variation with the azimuthal angle was obtained with respect to a rotational-axis system, $x_R O y_R$ where $x_R$ has its initial position linked to blade No.1 in Figure 2.

Figure 3 shows the resultant of the normal force coefficient for two blades as a function of the blade position. For a tip speed ratio of $X_{EQ}$= 3.0, the zero value of $F_N$ may be observed
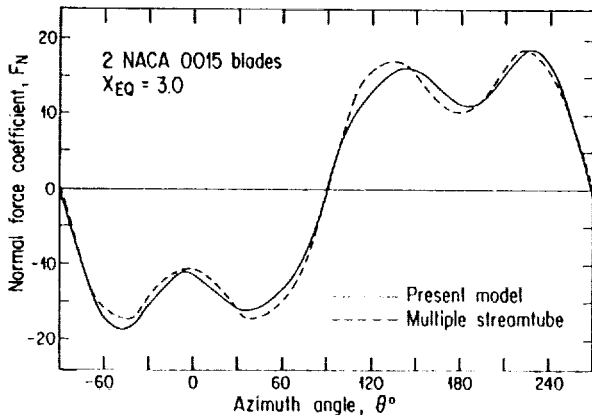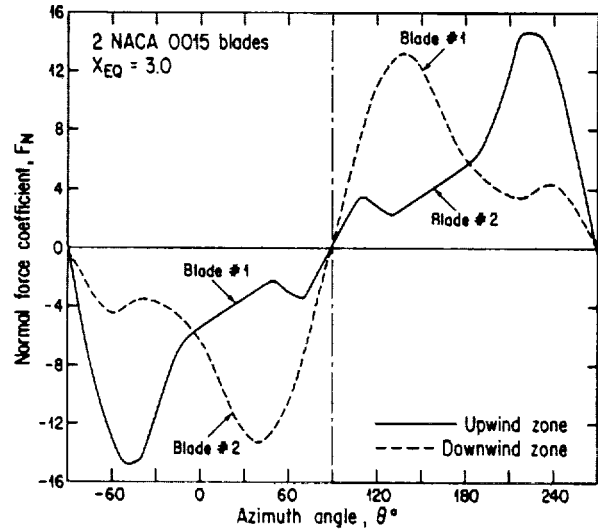


Figure 4 – Variation with azimuthal angle $\theta$ of the normal blade loading, for each blade, in the upwind and downwind zones.
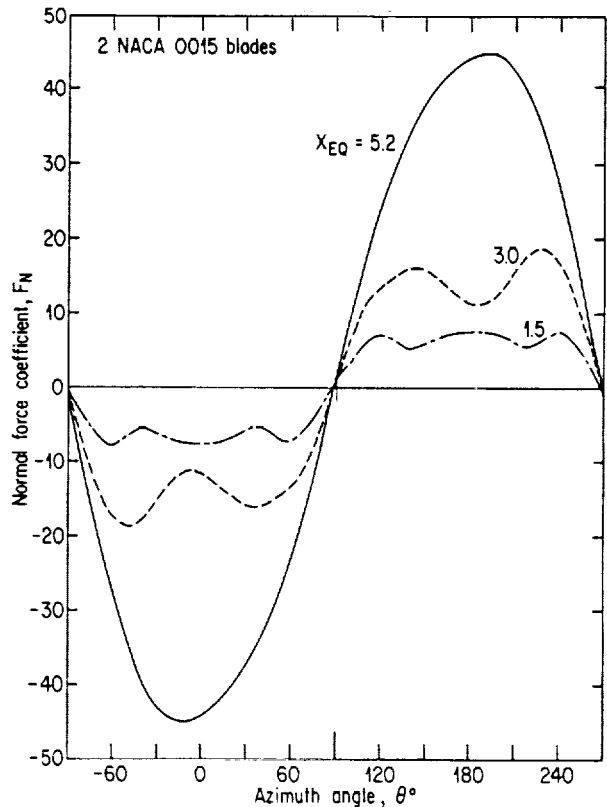


Figure 5 – Variation with azimuthal angle $\theta$ of the normal force coefficient, for two blades, at three tip speed ratios.

to occur at $\theta <$ 90° in contrast with $\theta = -$90°, as is the case of the multiple-streamtube model. The variation in the normal force coefficient with the blade position is shown in Figure 4 for each blade; the normal forces are smaller in the downwind than in the upwind zone. The effect of the tip speed ratio on the normal force is presented in Figure 5 for $X_{EQ}$ = 1.5, 3.0 and 5.2.
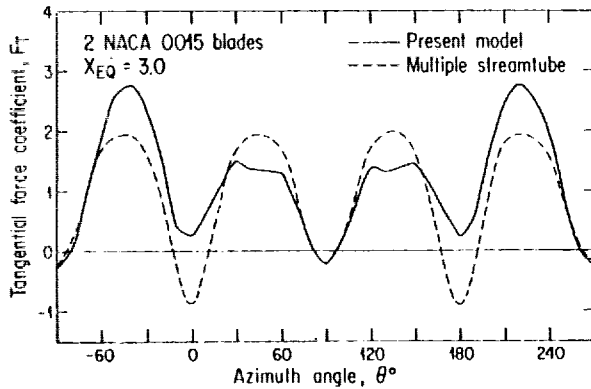


Figure 3 – Comparison between normal force coefficients calculated by the multiple-streamtube theory, and the present model.
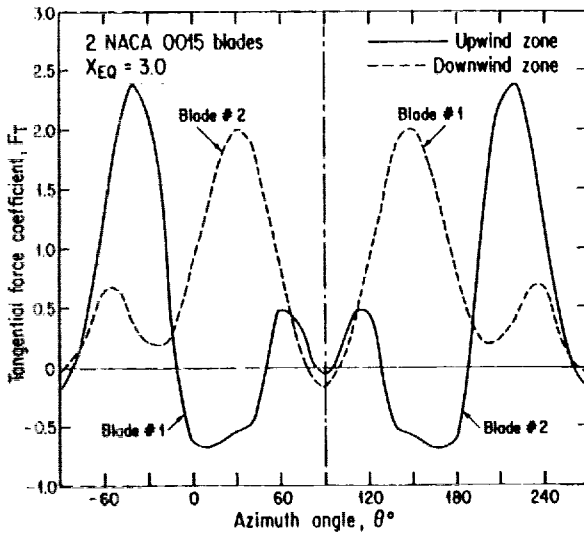
Figure 6 – Comparison between tangential force
coefficients calculated by the multi-
ple-streamtube theory and the present
model.



Figure 7 – Variation of the tangential blade
loading with the azimuthal angle $\theta$,
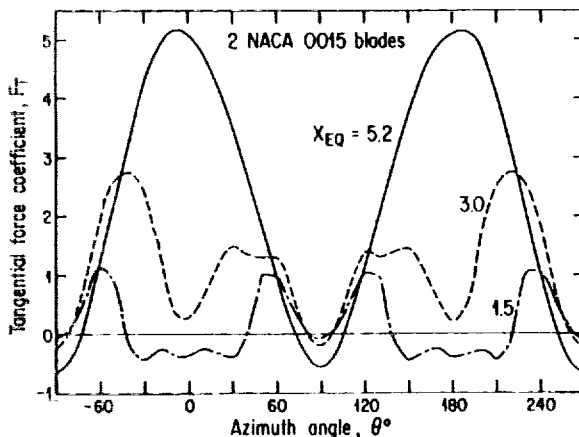for each blade, in the upwind and
downwind zones.



Figure 8 – Variation of the tangential force
coefficient with the azimuthal angle
$\theta$, for the two blades, at three tip
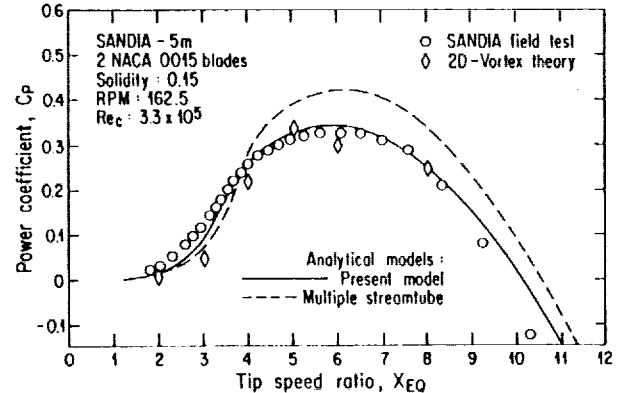speed ratios.



Figure 9 – Power coefficient as a function of
the equatorial tip speed ratio.
Comparison between analytical model
results and field test data for the
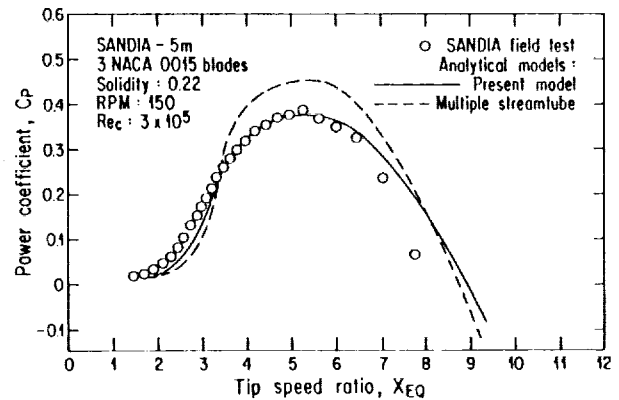Sandia 5-m, two-blade rotor.



Figure 10 – Power coefficient as a function of
the equatorial tip speed ratio.
Comparison between analytical model
results and field test data for the
Sandia 5-m, three-blade rotor.

The tangential force coefficient for two complete
blades as a function of the azimuthal angle is
plotted in Figure 6 for a tip speed ratio of
$X_{EQ} = 3.0$. The variation of this force calculat-
ed with multiple-streamtubes is similar on both
half-cycles of the rotor. The tangential forces
obtained with the present model are smaller on
the downwind face of the rotor in comparison with
the tangential forces on the upwind face, Figure
7. The effect of the tip speed ratio on the
tangential force is given in Figure 8 for
$X_{EQ} = 1.5$, 3.0 and 5.2.

Figure 9 presents a comparison of the power co-
efficient results from three analytical models:
multiple-streamtubes, two-dimensional vortex
theory and double-multiple-streamtubes with
Sandia field test data for two NACA-0015 blades,
5-m rotor. We can see that the double-multiple-
streamtube model is in good agreement with the
experimental data for tip speed ratios of 3.5 to
8.5. The results of the present model are better
than with other streamtube methods because the
downwind blade sees the induced velocity differ-
ently from the upwind blade, $V' < V$. This con-
cept can be improved by considering the effects

23

of the dynamic stall of the blades which is prevalent at low tip speed ratios and causes the torque to increase.

Figure 10 shows a comparison between the power coefficient obtained from the multiple-stream-tube theory, the present model and the Sandia field tests for three NACA-0015 blades, 5-m rotor. There is a good agreement with test data up to tip speed ratio of about 7; for low speed ratios, $X_{EQ} = 3.5$, the same phenomenon as with a two-blade rotor can be observed. There is a big difference between the multiple-streamtube results and experimental data, where the power coefficient reaches its maximum. The tip speed ratio for a maximum power coefficient decreases mainly with increasing drag and does not seem to be influenced by the number of blades. Retardation of the flow in both upstream and downstream zones intensifies with increasing rotor solidity; however, this effect is more significant in the downstream region of the rotor.

## CONCLUSION

The present analytical model represents an extension of the multiple-streamtube model, which is capable of calculating the difference in the induced velocities at the upstream and downstream passes. This is possible if it is assumed that each element of the rotor is replaced by two actuator disks in tandem, in the wind direction. The aerodynamic characteristics for each element of the blade were therefore obtained independently for the upwind and downwind parts of the rotor by using both the local Reynolds number and the local angle of attack.

The double-multiple-streamtube model allows for variation of the aerodynamic loads and the torque with the blade position for each part of the rotor. The method is generally adequate for studying a Darrieus rotor with several curved blades. Field test data with a Sandia 5-m machine and comparisons with previous methods satisfactorily confirm the theoretical predictions for the overall performance parameters.

The present model could be improved by considering the effect of dynamic stall on the blades, which would enhance the ability to predict both loads and performance. This refinement is currently under way at IREQ and the results will be compared with those furnished by other analytical models as well as with Magdalen Islands field test data.

## REFERENCES

1. Templin, R.J.: Aerodynamic Theory for the NRC Vertical-Axis Wind Turbine, NRC of Canada TR LTR-LA-160, 1974.

2. Strickland, J.H.: The Darrieus Turbine: A Performance Prediction Model Using Multiple Streamtubes, Sandia Laboratory Report SAND 75-0431, 1975.

3. Klimas, P.C.: Vertical Axis Wind Turbine Aerodynamic Performance Prediction Methods, Proceedings of the Vertical-Axis Wind Turbine (VAWT), Albuquerque, N.M., April 1-3, 1980.

4. Holme, O.: A Contribution to the Aerodynamic Theory of the Vertical-Axis Wind Turbine, International Symposium on Wind Energy Systems, Cambridge, England, September 1976.

5. Fanucci, J.B., and Walters, R.E.: Innovative Wind Machines: The Theoretical Performance of a Vertical-Axis Wind Turbine, Sandia Laboratory Report SAND 76-5586, p.III-61-93.

6. Strickland, J.H., Webster, B.T., and Nguyen, T.: A Vortex Model of the Darrieus Turbine: An Analytical and Experimental Study, Sandia Laboratory Report SAND 79-7058, 1980.

7. Lapin, E.E.: Theoretical Performance of Vertical-Axis Wind Turbines, ASME paper 75-WA/Ener-1, The Winter Annual Meeting, Houston, Texas, Nov. 30 - Dec. 4, 1975.

8. Sheldahl, R.E., Klimas, P.C., and Feltz, L.V.: Aerodynamic Performance of a 5-Metre-Diameter Darrieus Turbine with Extruded Aluminium NACA - 0015 Blades, Sandia Laboratory Report SAND 80-0179.

QUESTIONS AND ANSWERS

I. Paraschivoiu

From: Art Smith

Q: If the Darrieus produces a significant side force, is it not wrong to neglect the lateral component of velocity?

A: *No, because the effect of the lateral component of velocity is normally smaller than 10% of the freestream velocity (see Ref. 6); if the lateral component of velocity is considered the loads prediction will be better.*